

# Cost-Effective Label-free Node Classification with LLMs

Taiyan Zhang\*<sup>†</sup>  
 ShanghaiTech University  
 Institute of Computing Technology,  
 Chinese Academy of Sciences  
 zhangty2022@shanghaitech.edu.cn

Renchi Yang<sup>†</sup>  
 Hong Kong Baptist University  
 renchi@hkbu.edu.hk

Mingyu Yan<sup>‡</sup>  
 State Key Lab of Processors, Institute  
 of Computing Technology, Chinese  
 Academy of Sciences  
 University of Chinese Academy of  
 Sciences  
 yanmingyu@ict.ac.cn

Xiaochun Ye  
 State Key Lab of Processors, Institute  
 of Computing Technology, Chinese  
 Academy of Sciences  
 University of Chinese Academy of  
 Sciences  
 yexiaochun@ict.ac.cn

Dongrui Fan  
 State Key Lab of Processors, Institute  
 of Computing Technology, Chinese  
 Academy of Sciences  
 University of Chinese Academy of  
 Sciences  
 fandr@ict.ac.cn

Yurui Lai  
 Hong Kong Baptist University  
 csyrlai@comp.hkbu.edu.hi

## Abstract

*Graph neural networks* (GNNs) have emerged as go-to models for node classification in graph data due to their powerful abilities in fusing graph structures and attributes. However, such models strongly rely on adequate high-quality labeled data for training, which are expensive to acquire in practice. With the advent of large language models (LLMs), a promising way is to leverage their superb zero-shot capabilities and massive knowledge for node labeling. Despite promising results reported, this methodology either demands considerable queries to LLMs, or suffers from compromised performance caused by noisy labels produced by LLMs.

To remedy these issues, this work presents Cella, an active self-training framework that integrates LLMs into GNNs in a cost-effective manner. The design recipe of Cella is to iteratively identify small sets of “critical” samples using GNNs and extract informative pseudo-labels for them with both LLMs and GNNs as additional supervision signals to enhance model training. Particularly, Cella includes three major components: (i) an effective active node selection strategy for initial annotations; (ii) a judicious sample selection scheme to sift out the “critical” nodes based on label *disharmonicity* and *entropy*; and (iii) a label refinement module combining LLMs and GNNs with rewired topology. Our extensive experiments over five benchmark text-attributed graph datasets demonstrate that Cella significantly outperforms the state of the arts under the

same query budget to LLMs in terms of label-free node classification. In particular, on the *DBLP* dataset with 14.3k nodes, Cella is able to achieve a 8.08% conspicuous improvement in accuracy over the state-of-the-art at a cost of less than one cent.

## CCS Concepts

• **Computing methodologies** → **Neural networks**; • **Information systems** → **Graph-based data models**.

## Keywords

Graph Neural Network, Large Language Models, Label-free Node Classification

## ACM Reference Format:

Taiyan Zhang, Renchi Yang, Mingyu Yan, Xiaochun Ye, Dongrui Fan, and Yurui Lai. 2018. Cost-Effective Label-free Node Classification with LLMs. In . ACM, New York, NY, USA, 15 pages. <https://doi.org/XXXXXXXX.XXXXXXX>

## 1 Introduction

*Text-attributed graphs* (TAGs) [4] are an expressive data model used to represent textual entities and their complex interconnections. Such data structures are prevalent in real-world scenarios, including social networks, hyperlink graphs of web pages, transaction networks, etc., wherein nodes are endowed with user profiles, web page contents, or product descriptions. Node classification is a fundamental task over TAGs, which aims to classify the nodes in the graph into a number of predefined categories based on the graph structures and textual contents. This task finds extensive practical web applications, such as fake news detection [54], document categorization [76], item tagging [42], financial fraud monitoring [77], and many others [3, 25, 36].

In the past decade, *graph neural networks* (GNNs) [5, 13, 22, 27, 67, 70, 72] have become the dominant models for node classification, by virtue of their capabilities to capture complex dependencies and patterns in the graph and the interplay between connectivity and attributes. However, the efficacy of such models largely hinges on the availability of adequate node labels for training. In real life, high-quality labels are hard to acquire due to the need for

\*Work done while at HKBU.

<sup>†</sup>Both authors contributed equally to the paper.

<sup>‡</sup>Corresponding Author

Permission to make digital or hard copies of all or part of this work for personal or classroom use is granted without fee provided that copies are not made or distributed for profit or commercial advantage and that copies bear this notice and the full citation on the first page. Copyrights for components of this work owned by others than ACM must be honored. Abstracting with credit is permitted. To copy otherwise, or republish, to post on servers or to redistribute to lists, requires prior specific permission and/or a fee. Request permissions from [permissions@acm.org](mailto:permissions@acm.org).

Conference'17, July 2017, Washington, DC, USA

© 2018 ACM.

ACM ISBN 978-1-4503-XXXX-X/18/06

<https://doi.org/XXXXXXXX.XXXXXXX>

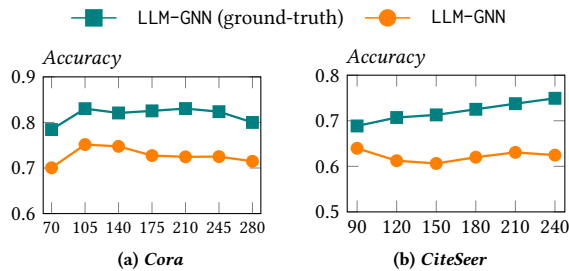


Figure 1: Varying #labeled nodes.

expert knowledge, significant human efforts, and potential biases in annotation, particularly for large-scale graphs comprising millions of nodes and a sheer volume of textual data [9, 53].

In light of the superb comprehension and reasoning abilities of *large language models* (LLMs) in dealing with textual data, LLMs have been employed as a powerful tool for analyzing TAGs. As manifested in [6, 20], LLMs have exhibited impressive node classification performance in TAGs under zero-shot or few-shot settings. However, compared to GNNs, this methodology falls short of exploiting the graph structures and requires substantial queries/calls to LLMs, and hence is not suitable for classifying nodes in the entire graph. Instead, a recent study [7] has made an attempt towards utilizing LLMs as annotators for node labeling to facilitate the zero-shot node classification over TAGs. In this pipeline, i.e., LLM-GNN, LLMs work as a front-mounted step to create labels for a small number of selected *active* nodes as training data, and subsequently, a GNN model is trained for classification with the labeled data.

Despite its empirical effectiveness as reported in [7], LLM-GNN is inherently defective due to its cascaded workflow that strongly relies on the active node selection and output quality of LLMs, which could be inaccurate/noisy, and in turn, leads to sub-optimal node classification performance. To illustrate, Figure 1 depicts the empirical performance attained by LLM-GNN and its variant whose active nodes are annotated with the ground-truth labels, dubbed as LLM-GNN (ground-truth), on two real TAGs (see Section 5), when increasing the labeled sample size. The first observation we can make from Figure 1 is that there is a notable performance gap (around 10%) between LLM-GNN and LLM-GNN (ground-truth). Second, as the labeled sample size, i.e., query budget for LLMs, is increased, LLM-GNN undergoes performance stagnation or even degradation on both datasets. These observations indicate that the label noise introduced by LLMs severely undermines the performance of GNNs. Moreover, even for LLM-GNN (ground-truth), we can also observe a drop of performance on *Cora* when training with more labeled data, which reveals the limitations of LLM-GNN in selecting representative active samples for labeling as well as vanilla GNN models.

To address the above-said problems, we present *Cella* (Cost-effective LLM-based label-free node classification), a new framework that integrates LLMs into GNNs for cost-effective zero-shot node classification. To achieve this goal, the basic idea of *Cella* is to actively capitalize on the rich structural and attribute semantics underlying the TAGs with GNNs and LLMs for active node selection, node annotation, and label correction, rather than solely based on LLMs. More concretely, *Cella* proceeds in two stages that both combine LLMs and GNNs. Given a total query budget  $B$  to access LLMs, the first stage in *Cella* pinpoints  $\varepsilon \cdot B$  ( $0 < \varepsilon < 1$ ) active

nodes for annotation by LLMs through the *subspace clustering* [61] based on GNN-based node representations, which enables the accurate selection of representative node samples with consideration of the inherent structures of the input graph and attribute data. The second stage resorts to a multi-round self-training pipeline, in which GNNs focus on identifying a set of “informative” samples with high-confidence and low-confidence labels using our proposed *label entropy* and *label disharmonicity* metrics, while the LLM is harnessed to generate more reliable labels for these uncertain samples with the remaining  $(1 - \varepsilon) \cdot B$  query budget. To reduce the label noise from LLMs, we further propose a *Dirichlet Energy*-based graph rewiring strategy to minimize the adverse effects of noisy or missing links in the original graphs, whereby *Cella* can infer new label predictions to refine the LLM-based annotations. The pseudo-labels for such informative samples will be further used as additional supervision signals to facilitate the subsequent model training.

To summarize, our contributions in this paper are as follows:

- We introduce a novel multi-round self-training framework that enables the cost-effective integration of LLMs and GNNs for improved label-free node classification.
- We propose an effective active node selection scheme for node annotations with LLMs.
- We design a judicious strategy for the selection of informative samples and a graph rewiring-based label refinement to create more reliable labeled data for model training.
- Extensive experiments comparing *Cella* against a total of 27 baselines over five real TAGs showcase that *Cella* can achieve a consistent and remarkable improvement of at least 5% in zero-shot classification accuracy compared to the state of the art in most cases.

## 2 Related Work

This section reviews existing studies germane to our work.

### 2.1 Zero-shot Node Classification

Zero-shot node classification aims to train a model on a set of known categories and generalize it to unseen categories. GraphCEN [26] introduces a two-level contrastive learning approach to jointly learn node embeddings and class assignments in an end-to-end fashion, effectively enabling the transfer of knowledge to unseen classes. Similarly, TAG-Z [30] leverages prompts alongside graph topology to generate preliminary logits, which can be directly applied to zero-shot node classification tasks. DGPN [65] facilitates zero-shot knowledge transfer by utilizing class semantic descriptions to transfer knowledge from seen to unseen categories, a process analogous to meta-learning. Additionally, methods such as BART [28] can also be adapted for node classification tasks. However, it is important to note that our approach differs slightly from traditional zero-shot node classification, as we do not require any initial training data.

## 2.2 Node Classification on Text-Attributed Graphs

Text-attributed graphs combine two modalities: the textual content within documents and the graph structure that connects these documents [4]. On the one hand, Graph Neural Networks (GNNs) [18] effectively generate document embeddings by integrating both vertex attributes and graph connectivity. However, most existing GNN-based models treat textual content as general attributes without specifically addressing the unique properties of language data. Consequently, they fail to capture the rich semantic structures and nuanced language representations embedded in text corpora.

On the other hand, pre-trained language models (PLMs) [59] and large language models (LLMs) excel at learning contextualized language representations and generating document embeddings. However, these models typically focus on individual documents and do not consider the graph connectivity between documents, such as citations or hyperlinks. This connectivity often encodes topic similarity, and by modeling it, one can propagate semantic information across connected documents.

To address these challenges, recent approaches have proposed text-attributed graph representation learning, which combines GNNs with PLMs and LLMs into unified frameworks for learning document embeddings that preserve both contextualized textual semantics and graph connectivity. For instance, Graphformers [78] iteratively integrate text encoding with graph aggregation, enabling each node’s semantics to be understood from a global perspective. GraphGPT [55] aligns LLMs with graph structures to improve document understanding. GraphAdapter [23] uses LLMs on graph-structured data with parameter-efficient tuning, yielding significant improvements in node classification. LLM-GNN [7] leverages LLMs to annotate node labels, which are subsequently used to train Graph Convolutional Networks (GCNs) in an instruction-tuning paradigm. OFA [34] introduces a novel graph prompting paradigm that appends prompting substructures to input graphs, enabling it to address various tasks, including node classification, without the need for fine-tuning. ZeroG [31] uses language models to encode both node attributes and class semantics, achieving significant performance improvements on node classification tasks.

These advancements in text-attributed graph methods have been successfully applied to a range of tasks, including text classification [66, 76], citation recommendation [2, 69], question answering [75], and document retrieval [41].

## 2.3 Attributed Graph Clustering

Attributed graph clustering (AGC) aims to effectively leverage both structural and attribute information in graphs for improved clustering performance [73]. Several key methods have been proposed in this domain. DAEGC [63] uses attention mechanisms to adaptively aggregate neighborhood information, improving the expressiveness of node embeddings. AGCN [46] dynamically blends attribute features from autoencoders (AE) with topological features from GCNs, using a heterogeneous fusion module to integrate both types of information. DFCN [58] combines representations from AE and GAE hidden layers through a fusion module and employs a triple self-supervision strategy to enhance cross-modal information utilization. CCGC [74] employs contrastive learning with non-shared

weight Siamese encoders to construct multiple views, improving the robustness and reliability of clustering through high-confidence semantic pairings. AGC-DRR [16], reduces redundant information in both input and latent spaces, enhancing the network’s robustness and feature discriminability.

## 2.4 Difference from Previous Works

In this section, we outline the key differences between our method and prior label-free approaches [7, 29]. Specifically, [7] employs traditional active selection techniques, such as FeatProp, RIM, and GraphPart, for node selection, performing annotation only once before the GNN training phase. In contrast, Cella introduces a novel subspace clustering approach and conducts annotation in batches throughout the self-training process. Additionally, Cella leverages reliable GNN predictions as pseudo-labels, thereby reducing the need for expensive LLM queries, and incorporates a Hybrid Label Refinement module to enhance the quality of node selection.

Ref. [29], while employing iterative node selection for annotation, initializes the process with random node selection, unlike our method, which utilizes subspace clustering. Furthermore, the selection metric defined in [29] differs significantly from ours. Lastly, their approach relies on the LLM to explain annotation decisions for knowledge distillation, which substantially increases the query cost, whereas Cella mitigates this by merely generating the annotation result with confidence.

## 3 Preliminaries

### 3.1 Problem Statement

Let  $\mathcal{G} = (\mathcal{V}, \mathcal{E}, \mathcal{T})$  be a *text-attributed graph*, wherein  $\mathcal{V}$  stands for a set of  $n$  nodes and  $\mathcal{E}$  represents a set of  $m$  edges between nodes in  $\mathcal{V}$ . For each edge  $(v_i, v_j) \in \mathcal{E}$ , we say  $v_i$  and  $v_j$  are neighbors to each other and use  $\mathcal{N}(v_i)$  to denote the set of neighbors of  $v_i$ . Each node  $v_i$  in  $\mathcal{G}$  is characterized by a text description  $T_i$  in  $\mathcal{T}$ . We denote by  $A$  the adjacency matrix of  $\mathcal{G}$ , in which  $A_{i,j} = A_{j,i} = 1$  if  $(v_i, v_j) \in \mathcal{E}$  and 0 otherwise. Accordingly,  $L = D - A$  is the Laplacian matrix of  $\mathcal{G}$ , where  $D$  is the diagonal degree matrix satisfying  $D_{i,i} = |\mathcal{N}(v_i)| \forall v_i \in \mathcal{V}$ .  $\tilde{A} = D^{-1/2} A D^{-1/2}$  stands for the normalized version of  $A$  and  $\tilde{L} = I - \tilde{A}$  is used to symbolize the normalized Laplacian of  $\mathcal{G}$ .

Let  $C = \{c_1, c_2, \dots, c_k\}$  be a set of  $k$  classes, where each class is associated with a label text. Given a TAG  $\mathcal{G} = (\mathcal{V}, \mathcal{E}, \mathcal{T})$  and  $k$  classes  $C$ , the goal of *label-free node classification* [7, 30] is to predict the class labels of *all* nodes in  $\mathcal{V}$ .

### 3.2 Graph Neural Networks

The majority of existing GNNs [5, 13, 27, 67, 70] mainly follow the *message passing* paradigm [15], which first aggregates features from the neighborhood, followed by a transformation. As demystified in recent studies [40, 80], after removing non-linear operations, graph convolutional layers in popular *graph neural network* models, e.g., APPNP [13], GCNII [5], and JKNet [70], essentially optimize the *graph Laplacian smoothing* [11] problem as formulated in Eq. (1).

$$\min_H (1 - \alpha) \cdot \|H - X\|_F^2 + \alpha \cdot \text{trace}(H^T \tilde{L} H), \quad (1)$$

where  $\alpha \in [0, 1]$  is a coefficient balancing two terms. The first term in Eq. (1) seeks to reduce the discrepancy between the input matrix  $X$  and the target node representations  $H$ . The second term calculates the *Dirichlet Energy* [8] of  $H$  over  $\mathcal{G}$ , which can be rewritten as  $\sum_{(v_i, v_j) \in \mathcal{E}} \left\| \frac{H_i}{\sqrt{d(v_i)}} - \frac{H_j}{\sqrt{d(v_j)}} \right\|_2^2$ , enforcing  $H_i, H_j$  of any adjacent nodes  $(v_i, v_j) \in \mathcal{E}$  to be close. By taking the derivative of Eq. (1) w.r.t.  $Z$  to zero and applying Neumann series [21], the closed-form solution (i.e., final node representations) can be expressed as

$$H = \sum_{t=0}^{\infty} (1 - \alpha) \alpha^t \tilde{A}^t X. \quad (2)$$

### 3.3 Large Language Models and Prompting

In this work, we refer to LLMs as the language models that have been pre-trained on extensive text corpora, which exhibit superb comprehension ability and massive knowledge at the cost of billions of parameters, such as LLaMA [57] and GPT4 [1]. The advent of LLMs has brought a new paradigm for task adaptation, which is known as “pre-train, prompt, and predict”. In such a paradigm, instead of undergoing cumbersome model fine-tuning on task-specific labeled data, the LLMs pre-trained on a large text corpus are queried with a natural language prompt specifying the task and context, and the models return the answer based on the instruction and the input text [35]. For example, given a paper titled “BERT: Pre-training of Deep Bidirectional Transformers for Language Understanding” and the task of predicting its subject. The prompts for this task can be:

{[Title], this, paper, belong, to, which, subject?}

While querying a model once with a reasonably sized input is affordable for most users, challenges arise when the input text is exceptionally long, such as a complete book or a lengthy article from a website. Additionally, the need to query large datasets further escalates costs. For instance, the PUBMED dataset contains tens of thousands of articles, with the longest exceeding 100,00 words. A full-scale prediction of all article subjects in the PUBMED dataset using GPT-3.5 could cost over 20 dollars, and with the more advanced GPT-4, this cost rises to around 400 dollars<sup>1</sup>.

Apart from incurring high costs, LLM predictions can sometimes be noisy. Although these models may exhibit high confidence in their outputs, they are prone to errors, a phenomenon often referred to as AI hallucination [48]. One potential solution to mitigate this issue is to experiment with different prompts and select the most accurate output. However, each attempt incurs significant costs due to the expensive nature of these models.

## 4 Methodology

This section presents our Cella framework that integrates LLMs into the GNNs adaptively for label-free node classification.

### 4.1 Synoptic Overview of Cella

The pipeline of Cella is illustrated in Figure 2, which mainly works in two stages: initial node annotations with LLMs (Stage I) and multi-round self-training based on GNNs (Stage II). More specifically, given a TAG  $\mathcal{G}$ , Cella first converts  $\mathcal{G}$  into a standard attributed

graph by encoding the text description  $T_i$  of each node  $v_i \in \mathcal{V}$  into a text embedding  $X_i \in \mathbb{R}^d$  as its attribute vector using PLMs, e.g., BERT [10] and Sentence-BERT [49].

Subsequently, Cella proceeds to the first stage, which seeks to create pseudo-labels  $\mathcal{Y}_{tr}$  for a small set  $\mathcal{V}_{tr}$  of nodes using LLMs as initial training samples. Given an allocated budget of  $B_{ini} = \varepsilon \cdot B$  ( $0 < \varepsilon \leq 1$ ) for querying LLMs, where  $B$  is the total query budget, Stage I extracts a small set  $\mathcal{A}$  of  $B_{ini}$  representative nodes from  $\mathcal{V}$  by our *active node selection strategy*, followed by carefully-designed prompts to LLMs for accurate annotations of samples in  $\mathcal{A}$ .

After that, Cella starts Stage II, which trains GNNs for  $R$  rounds by taking as input the graph  $\mathcal{G}$  with attribute matrix  $X$ , training samples  $(\mathcal{V}_{tr}, \mathcal{Y}_{tr})$ , and the remaining query budget of  $B_{ref} = (1 - \varepsilon) \cdot B$  to LLMs. In  $r$ -th ( $1 \leq r \leq R$ ) round of the self-training, Cella begins by generating current label predictions  $Y^{(r)} \in \mathbb{R}^{|\mathcal{V}| \times k}$  by a GNN model trained on  $(\mathcal{V}_{tr}, \mathcal{Y}_{tr})$ . With the class probabilities therefrom and the graph structures, our *informative sample selection* module first evaluates the *informativeness* of nodes in the test set  $\mathcal{V} \setminus \mathcal{V}_{tr}$  and then filter out two small sets  $\mathcal{V}_{ct}$  and  $\mathcal{V}_{ut}$  that comprise samples for which the current model is the most and least confident and about their class predictions, respectively. For the most uncertain samples in  $\mathcal{V}_{ut}$ , we resort to a *hybrid* approach for refining or rectifying their predicted labels, which effectively combines additional knowledge injected from LLMs and rewired graph topology. In the end, Cella expands  $\mathcal{V}_{tr}$  with  $\mathcal{V}_{ct}$  and  $\mathcal{V}_{ut}$  and enters into next round of self-training.

In what follows, we first introduce our strategies for selecting active nodes and querying LLMs for initial node annotations in Section 4.2. Sections 4.3 and 4.4 elaborate on the selection of informative samples and our hybrid label refinement scheme, respectively. In Sections 4.5 and 4.6, we describe the training objectives of Cella and conduct related analyses.

### 4.2 Initial Node Annotations

This stage involves the selection of nodes  $\mathcal{A}$  for annotation and specific labeling tricks using LLMs.

**4.2.1 Active Node Selection.** The basic idea of our node selection strategy is to partition nodes in  $\mathcal{V}$  into a number of clusters and select a small set  $\mathcal{A}$  ( $|\mathcal{A}| = B_{ini}$ ) of distinct cluster centers and nodes as the representatives for subsequent annotations, referred to as the *active node set* (ANS).

To extract ANS  $\mathcal{A}$ , we first calculate a  $T$ -truncated approximation of the GNN-based node representations in Eq. (2) by

$$H = \sum_{t=0}^T (1 - \alpha) \alpha^t \tilde{A}^t X \quad (3)$$

as the feature vectors of nodes, which encode both textual and structural semantics underlying  $\mathcal{G}$ . Next, Cella opts for the *subspace clustering* (SC) technique [61] for node grouping, which is powerful in noise reduction and discovering structural patterns underlying the feature vectors [12]. To be specific, SC first constructs an affinity graph (a.k.a. self-expressive matrix), i.e.,  $S$ , from feature vectors  $H$  such that the following objective is optimized:

$$\min_{S \in \mathbb{R}^{n \times n}} \|H - SH\|_F^2 + \Omega(S), \quad (4)$$

<sup>1</sup>Price estimates are based on gpt-3.5-turbo-16k-0613 and gpt-4-32k-0613 models.

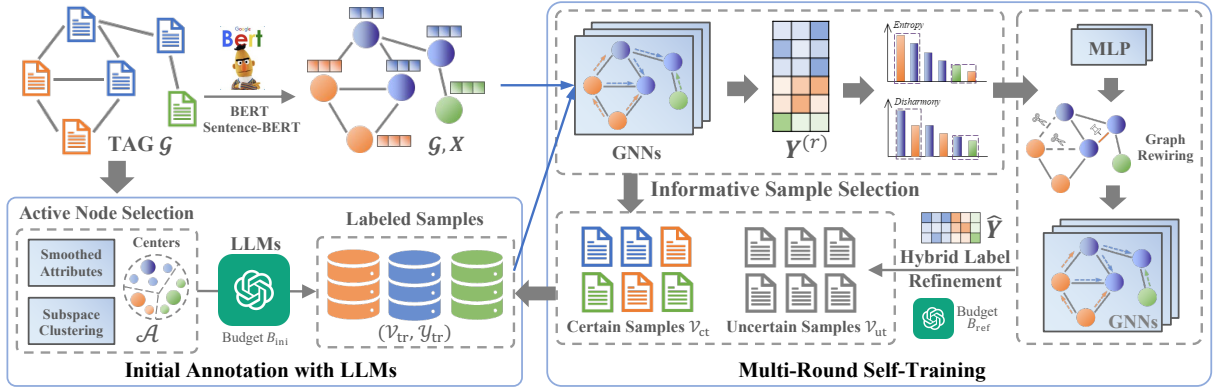


Figure 2: Pipeline of Our Proposed Cella

where  $\Omega(S)$  signifies a regularization term introduced to impose additional structure constraints on  $S$ . A popular choice for  $\Omega(S)$  is the nuclear norm  $\|S\|_*$ , which is to promote the low-rankness of  $S$  [33]. As such, if we let  $U$  be the left singular vectors of  $X$ , the minimizer of Eq. (4) is uniquely given by  $S = UU^T$  [33].

LEMMA 4.1. *The spectral clustering of  $S$  with  $K$  desired clusters is equivalent to applying the  $K$ -Means over  $U$ .*

Afterwards, standard SC applies the *spectral clustering* [62] over  $\frac{S+S^T}{2}$  to derive clusters. Lemma 4.1<sup>2</sup> establishes a connection between the spectral clustering of  $S$  and  $K$ -Means over  $U$ . Note that the exact construction of  $U$  entails prohibitive computational and space costs of  $O(|\mathcal{V}|^2)$ . As a partial remedy, we simplify the clustering as executing the  $K$ -Means with top- $\tau$  (typically  $\tau = 128$ ) left singular vectors  $U^{(\tau)}$  of  $X$ .

Denote by  $u_1, \dots, u_K \in \mathcal{V}$  the  $K$  centers obtained. We sort the remaining nodes in  $\mathcal{V} \setminus \{u_1, \dots, u_K\}$  in descending order by their closeness to their respective centers as defined in Eq. (5), and add the top  $B_{\text{ini}} - K$  ones together with  $u_1, \dots, u_K$  to ANS  $\mathcal{A}$ .

$$\frac{1}{1 + \left\| U_i^{(\tau)} - U_{u_j}^{(\tau)} \right\|_2} \quad (5)$$

The rationale is based on the observation from [7] indicating that nodes closer to cluster centers show higher quality and lower difficulty in annotation.

**4.2.2 LLM-based Annotation.** Given the ANS  $\mathcal{A}$ , Cella then query LLMs (e.g., GPT-3.5) for generating the annotation and confidence score for each node in  $\mathcal{A}$  using the *consistency prompt* strategy [64] adopted in [7]. Given these confidence scores, a post-filtering [7] is further applied to filter out the low-confidence samples with low-quality labels. Finally, we utilize the ANS  $\mathcal{A}$  and their annotations as the initial training data  $(\mathcal{V}_{\text{tr}}, \mathcal{Y}_{\text{tr}})$  input to the Cella model for self-training. We refer interested readers to Appendix B for detailed prompt descriptions and examples.

### 4.3 Informative Sample Selection

As delineated in Section 4.1, in the course of self-training, Cella selects node samples from the test node set  $\mathcal{V} \setminus \mathcal{V}_{\text{tr}}$  with high

<sup>2</sup>All missing proofs appear in Appendix A.

informativeness for the subsequent training based on the feedback provided by the past and current models trained with  $(\mathcal{V}_{\text{tr}}, \mathcal{Y}_{\text{tr}})$ .

Given the predictive probabilities in  $Y^{(r)}$  output by current model  $f^{(r)}$ ,  $\mathcal{V} \setminus \mathcal{V}_{\text{tr}}$  can be roughly categorized into three groups of node samples: *most certain samples*  $\mathcal{V}_{\text{ct}}$ , *most uncertain samples*  $\mathcal{V}_{\text{ut}}$ , and others. To be precise,  $\mathcal{V}_{\text{ct}}$  consists of nodes for which we are most certain about their label predictions in  $Y^{(r)}$ , while  $\mathcal{V}_{\text{ut}}$  includes the most uncertain ones. Intuitively, node samples in  $\mathcal{V}_{\text{ct}}$  and  $\mathcal{V}_{\text{ut}}$  are the most informative ones. The former can be used as additional supervision signals that guide the model towards accurate predictions, while the latter causes the performance *bottleneck* of the current model  $f^{(r)}$ , whose predictions are tentative due to data scarcity or limited model capacity. Accordingly, identifying such nodes for label refinement is crucial for upgrading the model. Next, we attend to constructing  $\mathcal{V}_{\text{ct}}$  and  $\mathcal{V}_{\text{ut}}$ . In particular, we set  $|\mathcal{V}_{\text{ct}}| = |\mathcal{V}_{\text{ut}}| = \frac{B_{\text{ref}}}{R-1}$ .

Firstly, we employ a GNN as the backbone  $f^{(r)}$ , followed by a softmax output layer, to obtain the new classification result:

$$Y^{(r)} = \text{softmax}(\text{GNN}(\mathcal{G}, X)). \quad (6)$$

To alleviate the model bias and sensitivity in each round and ensure a robust and accurate identification of  $\mathcal{V}_{\text{ct}}$  and  $\mathcal{V}_{\text{ut}}$ , we propose an ensemble scheme that averages the label predictions in past rounds to reach a consensus as follows:

$$\bar{Y}^{(r)} = \sum_{\ell=1}^r \frac{(1-\alpha)\alpha^\ell}{1-\alpha^r} Y^{(\ell)}, \quad (7)$$

where  $\frac{(1-\alpha)\alpha^\ell}{1-\alpha^r}$  stands for the weight assigned for the  $\ell$ -th round result, which decreases as  $\ell$  increases since intuitively initial predictions are less accurate than the latter ones. On its basis, we introduce two metrics, *label entropy* and *label disharmonicity*, to quantify the certainty or uncertainty of node samples.

**Label Entropy.** A simple and straightforward way is to adopt the prominent Shannon *entropy* [52] from the information theory to measure the uncertainty. Mathematically, the *label entropy* of a node  $v_i \in \mathcal{V} \setminus \mathcal{V}_{\text{tr}}$  can be formulated as

$$LE(v_i) = - \sum_{j=1}^k \bar{Y}_{i,j}^{(r)} \cdot \log(\bar{Y}_{i,j}^{(r)} + \sigma), \quad (8)$$

where  $\sigma$  (typically  $10^{-9}$ ) is introduced to avoid zero values. A high label entropy value connotes that the predicted probabilities are evenly distributed among all possible classes, and hence, indicates that the prediction is highly uncertain. Intuitively, the larger  $LE(v_i)$  is, the less confident we are about the label predictions for node  $v_i$ .

**Label Disharmonicity.** Note that the label entropy assesses the predictive outcome by merely inspecting the node-class relations in  $Y^{(r)}$ , which disregards the correlations between samples, i.e., topological connections in  $\mathcal{G}$ , and thus, engenders biased evaluation. To remedy its deficiency, we additionally introduce a novel notion of *label disharmonicity*. For each node  $v_i \in \mathcal{V} \setminus \mathcal{V}_{\text{tr}}$ , its label disharmonicity is defined by

$$LH(v_i) = \sqrt{\sum_{j=1}^k \left( \bar{Y}_{i,j}^{(r)} - \frac{1}{|\mathcal{N}(v_i)|} \sum_{v_t \in \mathcal{N}(v_i)} \bar{Y}_{t,j}^{(r)} \right)^2}, \quad (9)$$

which calculates the the discrepancy of  $v_i$ 's class labels from those of its neighbors in  $\mathcal{G}$ . Intuitively, the larger  $LH(v_i)$  is, the more unreliable the predicted label of  $v_i$  by  $\bar{Y}^{(r)}$  is.

**Constructions of  $\mathcal{V}_{\text{ct}}$  and  $\mathcal{V}_{\text{ut}}$ .** With the foregoing scores at hand, we create  $\mathcal{V}_{\text{ct}}$  as follows. Firstly, we extract two sets  $\mathcal{S}_{\text{har}}$  and  $\mathcal{S}_{\text{ent}}$  from  $\mathcal{V} \setminus \mathcal{V}_{\text{tr}}$  by

$$\mathcal{S}_{\text{har}} = \arg \text{topk}_{v_i \in \mathcal{V} \setminus \mathcal{V}_{\text{tr}}} -LH(v_i) \text{ and } \mathcal{S}_{\text{ent}} = \arg \text{topk}_{v_i \in \mathcal{V} \setminus \mathcal{V}_{\text{tr}}} LE(v_i), \quad (10)$$

where  $k = \frac{|B_{\text{ref}}|}{R-1}$  and  $\mathcal{S}_{\text{har}}$  (resp.  $\mathcal{S}_{\text{ent}}$ ) contains the nodes with  $\frac{|B_{\text{ref}}|}{R-1}$ -largest (resp. smallest) label entropy (resp. disharmonicity) in  $\mathcal{V} \setminus \mathcal{V}_{\text{tr}}$ . In turn, the set  $\mathcal{V}_{\text{ct}}$  can be formed via

$$\mathcal{V}_{\text{ct}} = (\mathcal{S}_{\text{har}} \cap \mathcal{S}_{\text{ent}}) \cup \bar{\mathcal{S}},$$

where  $\bar{\mathcal{S}}$  is a union of the remaining samples picked from  $\mathcal{S}_{\text{har}}$  and  $\mathcal{S}_{\text{ent}}$  with  $k = (|B_{\text{ref}}|/(R-1) - |\mathcal{S}_{\text{har}} \cap \mathcal{S}_{\text{ent}}|) / 2$  as follows:

$$\bar{\mathcal{S}} = \left( \arg \text{topk}_{v_i \in \mathcal{S}_{\text{har}} \setminus \mathcal{S}_{\text{ent}}} -LH(v_i) \right) \cup \left( \arg \text{topk}_{v_i \in \mathcal{S}_{\text{ent}} \setminus \mathcal{S}_{\text{har}}} LE(v_i) \right). \quad (11)$$

In a similar vein, we can obtain  $\mathcal{V}_{\text{ut}}$  by sorting the nodes in reverse orders, i.e., replacing  $-LH(v_i)$  and  $LE(v_i)$  in Eq. (10) and Eq. (11) by  $LH(v_i)$  and  $-LE(v_i)$ , respectively.

#### 4.4 Hybrid Label Refinement

As remarked in the preceding section,  $\mathcal{V}_{\text{ut}}$  consists of the bottleneck samples where the past and current GNN models largely fail. The uncertain predictions for samples in  $\mathcal{V}_{\text{ut}}$  can be ascribed to two primary causes. First, there is a lack of sufficient representative labeled samples for model training. Second, the nodes in  $\mathcal{V}_{\text{ut}}$  are connected to scarce or noisy edges that can easily mislead the GNN inference. Naturally, it is necessary to seek auxiliary label information from LLMs. However, as revealed in [7], the predictions made by LLMs can also be noisy, particularly for instances in  $\mathcal{V}_{\text{ut}}$  with low confidence. To mitigate this issue, we propose to rewire the graph structure surrounding the uncertain samples and re-train a GNN model to get their new predictions  $\hat{Y}^{(r)}$ . On top of that, we refine the labels of node samples in  $\mathcal{V}_{\text{ut}}$  through a careful combination of the signals from LLMs and  $\hat{Y}^{(r)}$ .

**4.4.1 Graph Rewiring-based Predictions.** To eliminate noisy topology and complete missing links, we propose to align the graph structure with the node features. Recall that in Eq. (1), GNNs aim to make node features  $\mathbf{H}$  optimize the Dirichlet Energy of node features over normalized graph Laplacian  $\tilde{\mathbf{L}}$ , thereby enforcing the feature vectors of adjacent nodes to be similar. Conversely, our idea is to optimize the Dirichlet Energy by updating  $\tilde{\mathbf{L}}$  while fixing  $\mathbf{H}$ .

LEMMA 4.2.  $I - \frac{1}{\beta} \cdot \mathbf{H}\mathbf{H}^T = \arg \min_{\tilde{\mathbf{L}}} \text{trace}(\mathbf{H}^T \tilde{\mathbf{L}} \mathbf{H})$  s.t.  $\|\tilde{\mathbf{A}}\|_F = \beta$ .

Along this line, we can obtain a new graph  $\mathcal{H}$  with adjacency matrix  $\mathbf{H}\mathbf{H}^T$  by Lemma 4.2. The connections therein can be used to complement the input graph topology in  $\mathcal{G}$ .

More concretely, Cella first generates the node feature through an MLP layer as follows:

$$\mathbf{H} = \text{MLP}(\mathcal{G}, Y^{(r)}).$$

The graph  $\mathcal{H}$  thus can be constructed by assigning each edge  $(v_i, v_j)$  a non-negative weight  $w(v_i, v_j)$  computed by

$$w(v_i, v_j) = \max(\mathbf{H}_i \cdot \mathbf{H}_j^T, 0).$$

As in Eq. (12), Cella forms (i) a set  $\mathcal{E}^{(-)}$  of edges to be removed from  $\mathcal{G}$ , and (ii) a set  $\mathcal{E}^{(+)}$  of node pairs to be connected in  $\mathcal{G}$ , by picking edges from  $\mathcal{E}$  with the  $\delta^{(-)} \cdot |\mathcal{E}|$ -smallest weights and node pairs from  $\mathcal{V}_{\text{tr}} \times \mathcal{V} \setminus \mathcal{V}_{\text{tr}}$  with the  $\delta^{(+)} \cdot |\mathcal{E}|$ -largest weights, respectively, where  $\delta^{(-)}$  and  $\delta^{(+)}$  are ratio parameters.

$$\mathcal{E}^{(-)} = \arg \text{topk}_{(v_i, v_j) \in \mathcal{E}} -w(v_i, v_j), \quad \mathcal{E}^{(+)} = \arg \text{topk}_{\substack{v_i \in \mathcal{V}_{\text{tr}}, v_j \in \mathcal{V} \setminus \mathcal{V}_{\text{tr}} \\ (v_i, v_i) \notin \mathcal{E}}} w(v_i, v_j). \quad (12)$$

The intuition for the way of creating  $\mathcal{E}^{(+)}$  is that by connecting unlabeled nodes to their similar samples with certain labels, the GNN model is empowered to infer their labels more accurately and confidently.

Then, we construct a rewired graph  $\hat{\mathcal{G}}$  with edge set  $(\mathcal{E} \cup \mathcal{E}^{(+)}) \setminus \mathcal{E}^{(-)}$  and derive an updated label predictions in Eq. (13) based thereon.

$$\hat{Y}^{(r)} = \text{softmax}(\text{GNN}(\hat{\mathcal{G}}, Y^{(r)})) \quad (13)$$

**4.4.2 Label Refinement with LLMs and  $\hat{Y}^{(r)}$ .** For each node  $v_i$  in  $\mathcal{V}_{\text{ut}}$ , Cella requests its annotation  $y_i$  with a confidence score  $\phi(v_i)$  from LLMs as in Section 4.2.2. Similarly, by  $\hat{Y}^{(r)}$  obtained in Eq. (13), we can get the most possible label  $\hat{y}_i$  for node  $v_i \in \mathcal{V}_{\text{ut}}$ . If  $y_i \neq \hat{y}_i$ , we should keep the one that we are more confident about. More precisely, let  $\text{rank}_{\text{LLM}}(v_i)$  and  $\text{rank}_{\text{GNN}}(v_i)$  be the rank of node  $v_i$  within  $\mathcal{V}_{\text{ut}}$  according to their confidence scores  $\phi(v_i)$  or prediction probabilities in  $\hat{Y}^{(r)}$ , respectively. Let  $\bar{\phi}$  be a predefined threshold, indicating the minimum confidence score to trust the result by LLMs. If  $\text{rank}_{\text{LLM}}(v_i) < \text{rank}_{\text{GNN}}(v_i)$  or  $\phi(v_i) \leq \bar{\phi}$ , Cella is less certain about the annotation by LLMs, and hence, we set  $\hat{y}_i$  as the final label for  $v_i$ .

#### 4.5 Model Optimization

In each round of self-training, we train the Cella model by optimizing two objectives pertinent to classification and rewired topology with the current training samples  $\mathcal{V}_{\text{tr}}$  and their labels  $\mathcal{Y}_{\text{tr}}$ . Following common practice, we adopt the *cross-entropy* loss for node

classification, which is formulated by

$$\mathcal{L}_{\text{CLS}} = \text{CrossEntropy}(Y_{\text{tr}}, \widehat{Y}_{\text{tr}}^{(r)}),$$

where  $Y_{\text{tr}}$  stands for the ground-truth labels for nodes in  $\mathcal{V}_{\text{tr}}$  and  $\widehat{Y}_{\text{tr}}^{(r)}$  contains the class probabilities of training samples predicted over the rewired graph  $\widehat{\mathcal{G}}$  as in Eq. (13).

To align with our objective of graph rewiring in Section (4.4.1), we additionally include the following loss:

$$\mathcal{L}_{\text{DE}} = \frac{|V|}{|E|} \cdot \left( \text{trace} \left( Y^{(r)\top} \tilde{L}_{\widehat{\mathcal{G}}} Y^{(r)} \right) - \lambda \cdot \|\tilde{L}_{\widehat{\mathcal{G}}}\|_F^2 \right), \quad (14)$$

where the first term measures the Dirichlet Energy of label predictions over the rewired graph  $\widehat{\mathcal{G}}$ , while the latter is the Tikhonov regularization [56] introduced to avoid trivial solutions.  $\lambda$  denotes the trade-off parameter between two terms.

## 4.6 Theoretical Analyses

**4.6.1 Connection between Label Disharmonicities and Dirichlet Energy.** Given a graph signal  $x \in \mathbb{R}^n$ , its standard Dirichlet Energy on  $\mathcal{G}$  is  $x^\top Lx$ , whose gradient can be expressed as  $Lx$ . Accordingly, for the probabilities of all nodes w.r.t.  $j$ -th class in  $\bar{Y}_{\cdot,j}^{(r)}$ , the gradient of its Dirichlet Energy is  $L\bar{Y}_{\cdot,j}^{(r)}$ , wherein each  $i$ -th entry equals  $\sum_{v_\ell \in \mathcal{N}(v_i)} \left( \bar{Y}_{i,j}^{(r)} - \bar{Y}_{\ell,j}^{(r)} \right)$ . As per the definition of the label disharmonicity in Eq. (9), it is easy to prove that  $LH(v_i) = \frac{1}{\sqrt{|\mathcal{N}(v_i)|}} \cdot \|(L\bar{Y}_{\cdot,j}^{(r)})_i\|_2$ . Namely, the label disharmonicity of a node  $v_i$  is the reweighted  $L_2$  norm of its Dirichlet Energy gradients of all classes over  $\mathcal{G}$ .

**4.6.2 Connection between  $\mathcal{L}_{\text{DE}}$  and Spectral Clustering.** Spectral clustering [62] seeks to partition nodes in graph  $\mathcal{G}$  into  $K$  disjoint clusters  $\{C_1, \dots, C_K\}$  such that their intra-cluster connectivity is minimized. A common formulation of such an objective is the RatioCut [17]:  $\min_{\{C_1, \dots, C_K\}} \sum_{k=1}^K \frac{1}{K} \sum_{v_i \in C_k, v_j \in \mathcal{V} \setminus C_k} \frac{\tilde{A}_{i,j}}{|C_k|}$ , which is equivalent to

$$\min_C \text{trace}(C^\top (I - \tilde{A})C) = \text{trace}(C^\top \tilde{L}C). \quad (15)$$

$C \in \mathbb{R}^{n \times K}$  denotes a node-cluster indicator matrix in which  $C_{i,j} = \frac{1}{\sqrt{|C_j|}}$  if  $v_i \in C_j$ , and 0 otherwise. This discreteness condition on  $C$  is usually relaxed in standard spectral clustering and  $C$  is allowed to be a continuous probability distribution. Let  $C = Y^{(r)}$  and  $\tilde{L} = \tilde{L}_{\widehat{\mathcal{G}}}$ . Our Dirichlet Energy term in Eq. (14) is a RatioCut in spectral clustering in essence.

## 5 Experiments

In this section, we experimentally evaluate Cella in label-free node classification over five real TAGs. Particularly, we investigate the following research questions: **RQ1:** How is the performance of Cella compared to the existing zero-shot/label-free methods? **RQ2:** How do the three proposed components of Cella affect its performance? **RQ3:** How do the key parameters in Cella affect its performance?

**Table 1: Dataset statistics.**

Dataset	#Nodes	#Edges	#Classes	Type
<i>Cora</i> [43]	2,708	5,429	7	Citation Graph
<i>Citeseer</i> [14]	3,186	4,277	6	Citation Graph
<i>Pubmed</i> [51]	19,717	44,335	3	Citation Graph
<i>WikiCS</i> [44]	11,701	215,863	10	Hyperlink Graph
<i>DBLP</i> [24]	14,376	431,326	4	Citation Graph

## 5.1 Experiment Settings

**Datasets and Metrics.** In this work, we use five benchmark TAG datasets for the node classification task, including *Cora*, *Citeseer*, *Pubmed*, *Wiki-CS*, and *DBLP*. The statistics of these datasets are provided in Table 1. Following prior works [7], we generate the attribute vector for each node using Sentence-BERT [49] as the text embedded to encode its associated text description. Four widely-used metrics [38]: *accuracy* (Acc), *normalized mutual information* (NMI), *adjusted Rand index* (ARI), and *F1-score* (F1), are adopted to assess the classification performance.

**Baselines.** For a comprehensive comparison, we evaluate Cella against seven categories of baseline approaches using various model architectures or backbones. Specifically, the first category uses MLP as the backbone, including LINK and LINKX [32], which are known for their powerful performance on graphs with low homophily. The second methodology involves BERT-like architectures and we choose five *pretrained language models* (PLMs): BERT [10], RoBERTa [37], DistilBERT [50], and DistilRoBERTa, and Sentence-BERT [49] with the *Sentence Embedding Similarity* metric. Additionally, we include BART-Large-MNLI [28], a pretrained model fine-tuned on the MNLI dataset. As for prompt engineering-based approaches, we go for two zero-shot prompt templates, i.e., zero-shot and zero-shot with Chain of Thought (COT), from Graph-LLM [6]. Furthermore, in the remaining three categories, we evaluate Cella with the state of the art, i.e., LLM-GNN [7], with three popular GNN models (GCN [27], GAT [60], and GCNII [5]) as the backbone, respectively. Particularly, for each category, we consider three variants of LLM-GNN with FeatProp (FP) [68], GraphPart (GP) [39], and RIM [79] as the active selection strategies.

**Other Settings.** All experiments are conducted on a Linux machine powered by an Intel Xeon Platinum 8352Y CPU with 128 cores, 2TB of host memory, and four NVIDIA A800 GPUs, each with 80GB of device memory. Unless otherwise specified, for the methods involving LLMs and GNNs, we employ *GPT-3.5-turbo* [1] as the LLM and adopt GCN [27] as the GNN backbone. For each dataset, the numbers of annotations from LLMs are ensured to be the same for all evaluated approaches. All reported results are averaged over three trials and each trial uses a different random seed for model training. For the interest of space, more details regarding datasets, baselines, and hyperparameters can be found in Appendix B.

## 5.2 RQ1. Comparison with Zero-Shot Methods

Table 2 presents the Acc, NMI, ARI, and F1 performance obtained by Cella and the aforementioned seven groups of baseline methods, i.e., 20 competitors, over the five datasets. Note that the LLM outputs by Graph-LLM [6] are invalid for F1-score calculation, and thus, are omitted. From Table 2, we can make the following observations.





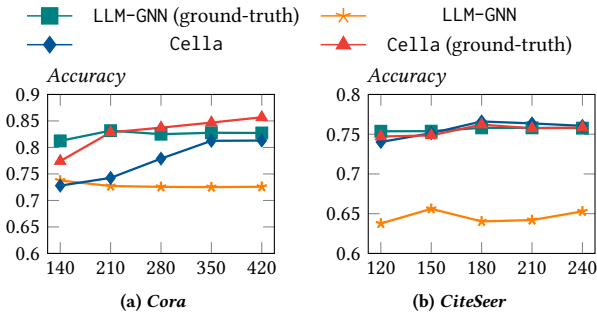


Figure 3: Varying  $B$  in Cella.

labels (dubbed as Cella (ground-truth) and LLM-GNN (ground-truth), respectively) when increasing the query budget  $B$  from 140 to 420, and from 120 to 240, on *Cora* and *CiteSeer*, respectively. It can be observed that the performance of Cella steadily improves as  $B$  increases. Particularly, compared to the approaches using ground-truth labels, Cella achieves matching performance on *CiteSeer*, and even higher accuracies on *Cora* when  $B \geq 280$ , demonstrating the effectiveness of our proposed techniques in utilizing GNNs for active node selection, node annotation, and label correction.

**Analysis of Budget Allocation Ratio  $\epsilon$ .** We further investigate how the budget allocation ratio  $\epsilon$  affects the performance of Cella, which determines the number of annotations used in the initial stage and subsequent self-training stages. Figure 4(a) depicts the Acc results of Cella when varying  $\epsilon$  from 0.1 to 0.9 on five datasets. We can observe that  $\epsilon$  has a remarkable impact on the model performance. In most cases, Cella obtains the best results when  $\epsilon$  is set to 0.5. The reason is that when the total budget is limited, a small  $\epsilon$  results in missing labeled samples in some categories, and hence, poor predictive performance. Conversely, if  $\epsilon$  is set too large, the annotated samples in the multi-round self-training phase will be significantly reduced, rendering Cella unable to adequately leverage the graph structures for label refinement but majorly dependent on noisy labels from LLMs. Therefore, setting  $\epsilon = 0.5$  leads to a favorable trade-off.

**Analysis of the Training Round  $R$ .** At last, we empirically study how the number  $R$  of rounds of self-training affects the performance of Cella. Figure 4(b) plots the classification accuracy of Cella when the number of rounds  $R$  is increased from 3 to 7. It can be observed that on all datasets, Cella first undergoes a performance rise, followed by a slight drop in accuracy, as increasing  $R$ . For instance, on small TAGs *Cora*, *CiteSeer*, and *PubMed*, Cella produces the best results when  $R = 5$ , while on larger datasets *WikiCS* and *DBLP*,  $R = 6$  is the best choice. Recall that given a fixed budget  $B$ , the query budget per round is  $\frac{B-B_{ini}}{R-1}$ . Consequently, increasing the rounds  $R$  leads to a smaller number of new annotated samples in each round, which is more likely to introduce label noise and hinder performance improvement.

Due to the space constraint, we defer to the results of additional parameters and other experiments to Appendix C.

## 6 Conclusion

In this work, we present Cella, a cost-effective solution that integrates LLMs into GNNs for label-free node classification. Cella

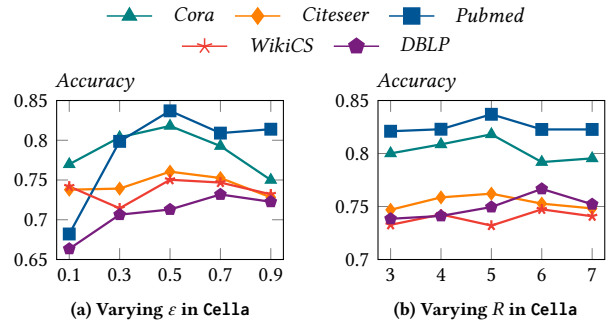


Figure 4: Varying  $R$  and  $\epsilon$  in Cella.

achieves high result utility through three major contributions: (i) an effective active node selection strategy for initial annotation via LLMs, (ii) a sample selection scheme that accurately identifies informative nodes based on our proposed label disharmonicity and entropy, and (iii) a label refinement module that combines the strengths of LLMs and GNNs with a rewired graph topology. Our extensive experiments over 5 real-world TAG datasets demonstrate the superiority of Cella over the state-of-the-art methods. In the future, we intend to scale Cella to large TAGs and extend it to other graph-related tasks or web applications, such as link prediction, graph classification, document categorization, and retrieval.

## References

- [1] Josh Achiam, Steven Adler, Sandhini Agarwal, Lama Ahmad, Ilge Akkaya, Florencia Leoni Aleman, Diogo Almeida, Janko Altenschmidt, Sam Altman, Shyamal Anadkat, et al. 2023. Gpt-4 technical report. *arXiv preprint arXiv:2303.08774* (2023).
- [2] Haoli Bai, Zhuangbin Chen, Michael R Lyu, Irwin King, and Zenglin Xu. 2018. Neural relational topic models for scientific article analysis. In *CIKM*. 27–36.
- [3] Smriti Bhagat, Graham Cormode, and S Muthukrishnan. 2011. Node classification in social networks. *Social network data analytics* (2011), 115–148.
- [4] Jonathan Chang and David Blei. 2009. Relational topic models for document networks. In *Artificial intelligence and statistics*. PMLR, 81–88.
- [5] Ming Chen, Zhewei Wei, Zengfeng Huang, Bolin Ding, and Yaliang Li. 2020. Simple and deep graph convolutional networks. In *International conference on machine learning*. PMLR, 1725–1735.
- [6] Zhikai Chen, Haitao Mao, Hang Li, Wei Jin, Hongzhi Wen, Xiaochi Wei, Shuaiqiang Wang, Dawei Yin, Wenqi Fan, Hui Liu, et al. 2024. Exploring the potential of large language models (llms) in learning on graphs. *ACM SIGKDD Explorations Newsletter* 25, 2 (2024), 42–61.
- [7] Zhikai Chen, Haitao Mao, Hongzhi Wen, Haoyu Han, Wei Jin, Haiyang Zhang, Hui Liu, and Jiliang Tang. 2023. Label-free Node Classification on Graphs with Large Language Models (LLMs). In *The Twelfth International Conference on Learning Representations*.
- [8] Fan RK Chung. 1997. *Spectral graph theory*. Vol. 92. American Mathematical Soc.
- [9] Anyan Dai, Charu Aggarwal, and Suhang Wang. 2021. NRGNN: Learning a Label Noise-Resistant Graph Neural Network on Sparsely and Noisily Labeled Graphs. arXiv:2106.04714 [cs.LG] <https://arxiv.org/abs/2106.04714>
- [10] Jacob Devlin, Ming-Wei Chang, Kenton Lee, and Kristina Toutanova. 2019. BERT: Pre-training of Deep Bidirectional Transformers for Language Understanding. arXiv:1810.04805 [cs.CL] <https://arxiv.org/abs/1810.04805>
- [11] Xiaowen Dong, Dorina Thanou, Pascal Frossard, and Pierre Vandergheynst. 2016. Learning Laplacian matrix in smooth graph signal representations. *IEEE Transactions on Signal Processing* 64, 23 (2016), 6160–6173.
- [12] Chakib Fettal, Lazhar Labiod, and Mohamed Nadif. 2023. Scalable attributed-graph subspace clustering. In *AAAI*, Vol. 37. 7559–7567.
- [13] Johannes Gasteiger, Aleksandar Bojchevski, and Stephan Günnemann. 2018. Predict then Propagate: Graph Neural Networks meet Personalized PageRank. In *International Conference on Learning Representations*.
- [14] C Lee Giles, Kurt D Bollacker, and Steve Lawrence. 1998. CiteSeer: An automatic citation indexing system. In *Proceedings of the third ACM conference on Digital libraries*. 89–98.
- [15] Justin Gilmer, Samuel S Schoenholz, Patrick F Riley, Oriol Vinyals, and George E Dahl. 2017. Neural message passing for quantum chemistry. In *International conference on machine learning*. PMLR, 1263–1272.

- [16] Lei Gong, Sihang Zhou, Wenxuan Tu, and Xinwang Liu. 2022. Attributed Graph Clustering with Dual Redundancy Reduction. In *IJCAI*. 3015–3021.
- [17] Lars Hagen and Andrew B Kahng. 1992. New spectral methods for ratio cut partitioning and clustering. *IEEE transactions on computer-aided design of integrated circuits and systems* 11, 9 (1992), 1074–1085.
- [18] Will Hamilton, Zhitao Ying, and Jure Leskovec. 2017. Inductive representation learning on large graphs. *NeurIPS* 30 (2017).
- [19] Jie Hao and William Zhu. 2023. Deep graph clustering with enhanced feature representations for community detection. *Applied Intelligence* 53, 2 (2023), 1336–1349.
- [20] Xiaoxin He, Xavier Bresson, Thomas Laurent, Adam Perold, Yann LeCun, and Bryan Hooi. 2024. Harnessing Explanations: LLM-to-LM Interpreter for Enhanced Text-Attributed Graph Representation Learning. In *ICLR*.
- [21] Roger A Horn and Charles R Johnson. 2012. *Matrix analysis*. Cambridge university press.
- [22] Keke Huang, Jing Tang, Juncheng Liu, Renchi Yang, and Xiaokui Xiao. 2023. Node-wise diffusion for scalable graph learning. In *TheWebConf*. 1723–1733.
- [23] Xuanwen Huang, Kaiqiao Han, Yang Yang, Dezheng Bao, Quanjin Tao, Ziwei Chai, and Qi Zhu. 2024. Can GNN be Good Adapter for LLMs? arXiv:2402.12984
- [24] Ming Ji, Yizhou Sun, Marina Danilevsky, Jiawei Han, and Jing Gao. 2010. Graph regularized transductive classification on heterogeneous information networks. In *Joint European Conference on Machine Learning and Knowledge Discovery in Databases*. Springer, 570–586.
- [25] Weiwei Jiang and Jiayun Luo. 2022. Graph neural network for traffic forecasting: A survey. *Expert systems with applications* 207 (2022), 117921.
- [26] Wei Ju, Yifang Qin, Siyu Yi, Zhengyang Mao, Kangjie Zheng, Luchen Liu, Xiao Luo, and Ming Zhang. 2023. Zero-shot node classification with graph contrastive embedding network. *Transactions on Machine Learning Research* (2023).
- [27] Thomas N Kipf and Max Welling. 2016. Semi-supervised classification with graph convolutional networks. *arXiv preprint arXiv:1609.02907* (2016).
- [28] Mike Lewis, Yinhan Liu, Naman Goyal, Marjan Ghazvininejad, Abdelrahman Mohamed, Omer Levy, Ves Stoyanov, and Luke Zettlemoyer. 2019. BART: Denoising Sequence-to-Sequence Pre-training for Natural Language Generation, Translation, and Comprehension. arXiv:1910.13461
- [29] Quan Li, Tianxiang Zhao, Lingwei Chen, Junjie Xu, and Suhang Wang. 2024. Enhancing Graph Neural Networks with Limited Labeled Data by Actively Distilling Knowledge from Large Language Models. arXiv:2407.13989
- [30] Yuexin Li and Bryan Hooi. 2023. Prompt-based zero-and few-shot node classification: A multimodal approach. *arXiv preprint arXiv:2307.11572* (2023).
- [31] Yuhan Li, Peisong Wang, Zhixun Li, Jeffrey Xu Yu, and Jia Li. 2024. ZeroG: Investigating Cross-dataset Zero-shot Transferability in Graphs. arXiv:2402.11235
- [32] Derek Lim, Felix Hohne, Xiuyu Li, Sijia Linda Huang, Vaishnavi Gupta, Omkar Bhalerao, and Ser-Nam Lim. 2021. Large Scale Learning on Non-Homophilous Graphs: New Benchmarks and Strong Simple Methods. arXiv:2110.14446
- [33] Guangcan Liu, Zhouchen Lin, and Yong Yu. 2010. Robust subspace segmentation by low-rank representation. In *Proceedings of the 27th international conference on machine learning (ICML-10)*. 663–670.
- [34] Hao Liu, Jiarui Feng, Lecheng Kong, Ningyue Liang, Dacheng Tao, Yixin Chen, and Muhan Zhang. 2024. One for All: Towards Training One Graph Model for All Classification Tasks. arXiv:2310.00149
- [35] Pengfei Liu, Weizhe Yuan, Jinlan Fu, Zhengbao Jiang, Hiroaki Hayashi, and Graham Neubig. 2023. Pre-train, prompt, and predict: A systematic survey of prompting methods in natural language processing. *Comput. Surveys* 55, 9 (2023), 1–35.
- [36] Yang Liu, Xiang Ao, Zidi Qin, Jianfeng Chi, Jinghua Feng, Hao Yang, and Qing He. 2021. Pick and choose: a GNN-based imbalanced learning approach for fraud detection. In *Proceedings of the Web conference*. 3168–3177.
- [37] Yinhan Liu, Myle Ott, Naman Goyal, Jingfei Du, Mandar Joshi, Danqi Chen, Omer Levy, Mike Lewis, Luke Zettlemoyer, and Veselin Stoyanov. 2019. RoBERTa: A Robustly Optimized BERT Pretraining Approach. arXiv:1907.11692
- [38] Yue Liu, Wenxuan Tu, Sihang Zhou, Xinwang Liu, Linxuan Song, Xihong Yang, and En Zhu. 2022. Deep graph clustering via dual correlation reduction. In *Proceedings of the AAAI conference on artificial intelligence*, Vol. 36. 7603–7611.
- [39] Jiaqi Ma, Ziqiao Ma, Joyce Chai, and Qiaozhu Mei. 2022. Partition-based active learning for graph neural networks. *arXiv preprint arXiv:2201.09391* (2022).
- [40] Yao Ma, Xiaorui Liu, Tong Zhao, Yozen Liu, Jiliang Tang, and Neil Shah. 2020. A Unified View on Graph Neural Networks as Graph Signal Denoising. *Proceedings of the International Conference on Information & Knowledge Management* (2020).
- [41] Zhengyi Ma, Zhicheng Dou, Wei Xu, Xinyu Zhang, Hao Jiang, Zhao Cao, and Ji-Rong Wen. 2021. Pre-training for ad-hoc retrieval: hyperlink is also you need. In *CIKM*. 1212–1221.
- [42] Kelong Mao, Xi Xiao, Jieming Zhu, Biao Lu, Ruiming Tang, and Xiuqiang He. 2020. Item tagging for information retrieval: A tripartite graph neural network based approach. In *Proceedings of the 43rd International ACM SIGIR Conference on Research and Development in Information Retrieval*. 2327–2336.
- [43] Andrew Kachites McCallum, Kamal Nigam, Jason Rennie, and Kristie Seymore. 2000. Automating the construction of internet portals with machine learning. *Information Retrieval* 3 (2000), 127–163.
- [44] Péter Mernyei and Cătălina Cangea. 2020. Wiki-cs: A wikipedia-based benchmark for graph neural networks. *arXiv preprint arXiv:2007.02901* (2020).
- [45] Péter Mernyei and Cătălina Cangea. 2022. Wiki-CS: A Wikipedia-Based Benchmark for Graph Neural Networks. arXiv:2007.02901
- [46] Zhihao Peng, Hui Liu, Yuheng Jia, and Junhui Hou. 2021. Attention-driven graph clustering network. In *MM*. 935–943.
- [47] Michael D Plummer and László Lovász. 1986. *Matching theory*. Elsevier.
- [48] Vipula Rawte, Amit Sheth, and Amitava Das. 2023. A survey of hallucination in large foundation models. *arXiv preprint arXiv:2309.05922* (2023).
- [49] Nils Reimers and Iryna Gurevych. 2019. Sentence-BERT: Sentence Embeddings using Siamese BERT-Networks. arXiv:1908.10084
- [50] Victor Sanh, Lysandre Debut, Julien Chaumond, and Thomas Wolf. 2019. DistilBERT, a distilled version of BERT: smaller, faster, cheaper and lighter. *ArXiv abs/1910.01108* (2019).
- [51] Prithviraj Sen, Galileo Namata, Mustafa Bilgic, Lise Getoor, Brian Gallagher, and Tina Eliassi-Rad. 2008. Collective classification in network data. *AI magazine* 29, 3 (2008), 93–93.
- [52] Claude Elwood Shannon. 1948. A mathematical theory of communication. *The Bell system technical journal* 27, 3 (1948), 379–423.
- [53] Victor S Sheng, Foster Provost, and Panagiotis G Ipeirotis. 2008. Get another label? improving data quality and data mining using multiple, noisy labelers. In *SIGKDD*. 614–622.
- [54] Chenguang Song, Kai Shu, and Bin Wu. 2021. Temporally evolving graph neural network for fake news detection. *Information Processing & Management* 58, 6 (2021), 102712.
- [55] Jiabin Tang, Yuhao Yang, Wei Wei, Lei Shi, Lixin Su, Suqi Cheng, Dawei Yin, and Chao Huang. 2024. GraphGPT: Graph Instruction Tuning for Large Language Models. arXiv:2310.13023
- [56] Andrey Nikolayevich Tikhonov. 1977. Solutions of Ill-Posed Problems. *VH Winston and Sons* (1977).
- [57] Hugo Touvron, Thibaut Lavril, Gautier Izacard, Xavier Martinet, Marie-Anne Lachaux, Timothée Lacroix, Baptiste Rozière, Naman Goyal, Eric Hambro, Faisal Azhar, et al. 2023. Llama: Open and efficient foundation language models. *arXiv preprint arXiv:2302.13971* (2023).
- [58] Wenxuan Tu, Sihang Zhou, Xinwang Liu, Xifeng Guo, Zhiping Cai, En Zhu, and Jieren Cheng. 2021. Deep fusion clustering network. In *Proceedings of the AAAI Conference on Artificial Intelligence*, Vol. 35. 9978–9987.
- [59] A Vaswani. 2017. Attention is all you need. *Advances in Neural Information Processing Systems* (2017).
- [60] Petar Veličković, Guillem Cucurull, Arantxa Casanova, Adriana Romero, Pietro Lio, and Yoshua Bengio. 2017. Graph attention networks. *arXiv preprint arXiv:1710.10903* (2017).
- [61] René Vidal. 2011. Subspace clustering. *IEEE Signal Processing Magazine* 28, 2 (2011), 52–68.
- [62] Ulrike Von Luxburg. 2007. A tutorial on spectral clustering. *Statistics and computing* 17 (2007), 395–416.
- [63] Chun Wang, Shirui Pan, Ruiqi Hu, Guodong Long, Jing Jiang, and Chengqi Zhang. 2019. Attributed graph clustering: A deep attentional embedding approach. *arXiv preprint arXiv:1906.06532* (2019).
- [64] Xuezhi Wang, Jason Wei, Dale Schuurmans, Quoc V Le, Ed H Chi, Sharan Narang, Aakanksha Chowdhery, and Denny Zhou. 2023. Self-Consistency Improves Chain of Thought Reasoning in Language Models. In *The Eleventh International Conference on Learning Representations*.
- [65] Zheng Wang, Jialong Wang, Yuchen Guo, and Zhiguo Gong. 2021. Zero-shot node classification with decomposed graph prototype network. In *Proceedings of the 27th ACM SIGKDD conference on knowledge discovery & data mining*. 1769–1779.
- [66] Zhihao Peng and Yuan Fang. 2023. Augmenting low-resource text classification with graph-grounded pre-training and prompting. In *SIGIR*. 506–516.
- [67] Felix Wu, Amauri Souza, Tianyi Zhang, Christopher Fifty, Tao Yu, and Kilian Weinberger. 2019. Simplifying graph convolutional networks. In *International conference on machine learning*. PMLR, 6861–6871.
- [68] Yuexin Wu, Yichong Xu, Aarti Singh, Yiming Yang, and Artur Dubrawski. 2019. Active learning for graph neural networks via node feature propagation. *arXiv preprint arXiv:1910.07567* (2019).
- [69] Qianqian Xie, Yutao Zhu, Jimin Huang, Pan Du, and Jian-Yun Nie. 2021. Graph neural collaborative topic model for citation recommendation. *ACM Transactions on Information Systems (TOIS)* 40, 3 (2021), 1–30.
- [70] Keyulu Xu, Chengtao Li, Yonglong Tian, Tomohiro Sonobe, Ken-ichi Kawarabayashi, and Stefanie Jegelka. 2018. Representation learning on graphs with jumping knowledge networks. In *International conference on machine learning*. 5453–5462.
- [71] Xiongfeng Yan, Tinghua Ai, Min Yang, and Xiaohua Tong. 2021. Graph convolutional autoencoder model for the shape coding and cognition of buildings in maps. *International Journal of Geographical Information Science* 35, 3 (2021), 490–512.
- [72] Renchi Yang, Jieming Shi, Xiaokui Xiao, Yin Yang, Sourav S Bhowmick, and Juncheng Liu. 2023. PANE: scalable and effective attributed network embedding. *The VLDB Journal* 32, 6 (2023), 1237–1262.

- [73] Renchi Yang, Jieming Shi, Yin Yang, Keke Huang, Shiqi Zhang, and Xiaokui Xiao. 2021. Effective and scalable clustering on massive attributed graphs. In *TheWebConf*. 3675–3687.
- [74] Xihong Yang, Yue Liu, Sihang Zhou, Siwei Wang, Wenxuan Tu, Qun Zheng, Xinwang Liu, Liming Fang, and En Zhu. 2023. Cluster-guided contrastive graph clustering network. In *Proceedings of the AAAI conference on artificial intelligence*, Vol. 37. 10834–10842.
- [75] Michihiro Yasunaga, Jure Leskovec, and Percy Liang. 2022. Linkbert: Pretraining language models with document links. *arXiv preprint arXiv:2203.15827* (2022).
- [76] Delvin Ce Zhang and Hady W Lauw. 2021. Semi-supervised semantic visualization for networked documents. In *Machine Learning and Knowledge Discovery in Databases. Research Track: European Conference, ECML PKDD 2021, Bilbao, Spain, September 13–17, 2021, Proceedings, Part III 21*. Springer, 762–778.
- [77] Ge Zhang, Zhao Li, Jiaming Huang, Jia Wu, Chuan Zhou, Jian Yang, and Jianliang Gao. 2022. e-fraudcom: An e-commerce fraud detection system via competitive graph neural networks. *TOIS* 40, 3 (2022), 1–29.
- [78] Jiawei Zhang, Haopeng Zhang, Congying Xia, and Li Sun. 2020. Graph-bert: Only attention is needed for learning graph representations. *arXiv preprint arXiv:2001.05140* (2020).
- [79] Wentao Zhang, Yexin Wang, Zhenbang You, Meng Cao, Ping Huang, Jiulong Shan, Zhi Yang, and Bin Cui. 2021. Rim: Reliable influence-based active learning on graphs. *NeurIPS* 34 (2021), 27978–27990.
- [80] Meiqi Zhu, Xiao Wang, Chuan Shi, Houye Ji, and Peng Cui. 2021. Interpreting and Unifying Graph Neural Networks with An Optimization Framework. *Proceedings of the Web Conference 2021* (2021).

## A Theoretical Proofs

**Proof of Lemma 4.1.** Let  $\{C_1, \dots, C_K\}$  be the  $K$  clusters and  $C \in \mathbb{R}^{|\mathcal{V}| \times K}$  be a node-cluster indicator wherein  $C_{i,k} = \frac{1}{\sqrt{|C_k|}}$  if  $v_i \in C_k$ , and 0 otherwise. Recall that the spectral clustering of affinity graph  $\frac{S+S^\top}{2} = S$  is to find  $C$  such that the following objective is optimized:

$$\max_C \text{trace}(C^\top S C). \quad (16)$$

Next, recall that  $K$ -Means seeks to minimize the Euclidean distance between data points and their respective cluster centroids, which leads to

$$\begin{aligned} & \min_C \sum_k \sum_{v_i \in C_k} \left\| U_i - \frac{1}{|C_k|} \sum_{v_j \in C_k} U_j \right\|_2^2 \\ &= \sum_k \sum_{v_i \in C_k} \|U_i\|_2^2 - \sum_k \sum_{v_j, v_\ell \in C_k} \frac{U_j \cdot U_\ell}{|C_k|} \\ &= \sum_k \sum_{v_i \in C_k} \|U_i\|_2^2 - \text{trace}(C^\top U U^\top C). \end{aligned}$$

Since the first term  $\sum_k \sum_{v_i \in C_k} \|U_i\|_2^2$  is fixed, the above optimization objective is equivalent to maximizing  $\text{trace}(C^\top U U^\top C)$ , which finishes the proof as  $S = U U^\top$ .  $\square$

**Proof of Lemma 4.2.** Recall that  $\tilde{L} = I - \tilde{A}$  in Section 3.1. Accordingly, the objective of  $\min_{\tilde{L}} \text{trace}(H^\top \tilde{L} H)$  is equivalent to optimizing  $\max_{\tilde{A}} \text{trace}(H^\top \tilde{A} H)$ .

Next, we rewrite  $\text{trace}(H^\top \tilde{A} H)$  as  $\text{trace}(\tilde{A} H H^\top)$  using the cyclic property of the trace. Based on the definition of matrix trace and Cauchy-Schwarz inequality,

$$\begin{aligned} \text{trace}(\tilde{A} H H^\top) &= \sum_{i,j=1}^n \tilde{A}_{i,j} \cdot (H H^\top)_{j,i} \\ &\leq \sqrt{\sum_{i,j=1}^n \tilde{A}_{i,j}^2} \cdot \sqrt{\sum_{i,j=1}^n (H H^\top)_{j,i}^2} \\ &= \|\tilde{A}\|_F \cdot \sqrt{\sum_{i,j=1}^n (H H^\top)_{j,i}^2} \\ &= \frac{1}{\beta} \cdot \sqrt{\sum_{i,j=1}^n (H H^\top)_{j,i}^2}. \end{aligned}$$

The maximum can be achieved when  $\tilde{A}_{j,i} = \frac{1}{\beta} \cdot (H H^\top)_{j,i}$ , which completes the proof.  $\square$

## B Experimental Details

### B.1 Details of the Prompt

In this section, we present the prompts designed for annotation with two examples. For *Cora*, *Citeseer*, *Pubmed*, and *WikiCS*, we incorporate label reasoning. Given that the reasoning text adds only a minimal cost compared to the longer query text in these datasets, its inclusion is acceptable and can slightly improve performance. However, for *DBLP*, where the query text is short, we did not include additional reasoning text. Tables 4 and 5 show the complete structure of our prompts. Specially, for *WikiCS*, we truncate the

text of the input article and make sure the total prompt is less than 4096 tokens.

**Table 4: Full prompt example for zero-shot annotation with a confidence score for *Pubmed***

---

#### Input:

You are a model that is especially good at classifying a paper's category. Now I will first give you all the possible categories and their explanations. Please answer the following question: What is the category of the target paper?

**All possible categories:** [Diabetes Mellitus Experimental, Diabetes Mellitus Type 1, Diabetes Mellitus Type 2]

**Category explanation:** Diabetes Mellitus Experimental: General experimental studies on diabetes, including comparisons across different animal models.

Diabetes Mellitus Type 1: Studies specific to Type 1 diabetes, involving metabolic changes and skeletal muscle metabolism.

Diabetes Mellitus Type 2: Studies specific to Type 2 diabetes, often involving complications, metabolic studies, and preventive measures.

#### Target paper:

**Title:** Isolated hyperglycemia at 1 hour on oral glucose tolerance test in pregnancy resembles gestational diabetes mellitus in predicting postpartum metabolic dysfunction.

**Abstract:** OBJECTIVE: Gestational impaired glucose tolerance (GIGT), defined by a single abnormal value on antepartum 3-h oral glucose tolerance test (OGTT) ... CONCLUSIONS: Like GDM, 1-h GIGT is associated with postpartum glycemia, insulin resistance, and beta-cell dysfunction.

Output your answer together with a confidence score ranging from 0 to 100, in the form of a list of Python dicts like ["answer": <answer\_here>, "confidence": <confidence\_here>]. You only need to output the one answer you think is the most likely.

#### Output:

---

**Table 5: Full prompt example for zero-shot annotation with a confidence score for *DBLP***

---

#### Input:

You are a model that is especially good at classifying a paper's category. Now I will first give you all the possible categories and their explanations. Please answer the following question: What is the category of the target paper?

**All possible categories:** [Database, Data Mining, AI, Information Retrieval]

#### Target Paper:

**Title:** Panel: User Modeling and User Interfaces.

Output your answer together with a confidence score ranging from 0 to 100, in the form of a list of Python dicts like ["answer": <answer\_here>, "confidence": <confidence\_here>]. You only need to output the one answer you think is the most likely.

#### Output:

---

**Table 6: Dataset descriptions.**

Dataset	#Nodes	#Edges	Task Description	Classes
<i>Cora</i>	2,708	5,429	Given the title and abstract, predict the category of this paper	Rule Learning, Neural Networks, Case Based, Genetic Algorithms, Theory, Reinforcement Learning, Probabilistic Methods
<i>Citeseer</i>	3,186	4,277	Given the title and abstract, predict the category of this paper	Agents, Machine Learning, Information Retrieval, Database, Human Computer Interaction, Artificial Intelligence
<i>Pubmed</i>	19,717	44,335	Given the title and abstract, predict the category of this paper	Diabetes Mellitus Experimental, Diabetes Mellitus Type 1, Diabetes Mellitus Type 2
<i>WikiCS</i>	11,701	215,863	Given the contents of the Wikipedia article, predict the category of this article	Computational linguistics, Databases, Operating systems, Computer architecture, Computer security, Internet protocols, Computer file systems, Distributed computing architecture, Web technology, Programming language topics
<i>DBLP</i>	14,376	431,326	Given the title of the paper in dblp database, predict the category of the paper	Database, Data Mining, AI, Information Retrieval

**Table 7: Hyperparameters for Cella with GCN, GAT, and GCNII backbones.**

	GCN					GAT					GCNII				
	<i>Cora</i>	<i>Citeseer</i>	<i>Pubmed</i>	<i>WikiCS</i>	<i>DBLP</i>	<i>Cora</i>	<i>Citeseer</i>	<i>Pubmed</i>	<i>WikiCS</i>	<i>DBLP</i>	<i>Cora</i>	<i>Citeseer</i>	<i>Pubmed</i>	<i>WikiCS</i>	<i>DBLP</i>
lr	0.01	0.01	0.01	0.01	0.1	0.01	0.01	0.01	0.01	0.1	0.01	0.01	0.01	0.01	0.05
dropout	0.5	0.5	0.5	0.5	0.5	0.5	0.5	0.2	0.5	0.5	0.5	0.5	0.5	0.5	0.5
#layers	2	2	2	2	2	2	2	2	2	2	64	32	16	8	2
hidden dim.	64	64	64	64	64	64	64	16	64	64	64	64	64	64	64
$T$	2	2	2	2	2	2	2	2	2	2	2	2	2	2	2
$\alpha$	1	1	1.2	1	1	1	1	1.2	1	1	1	1	1.2	1	1
$\epsilon$	0.5	0.4	0.5	0.4	0.25	0.4	0.4	0.5	0.3	0.4	0.4	0.33	0.5	0.4	0.3
$\tau$	128	128	256	256	64	128	128	4	128	32	128	256	4	128	128
$\lambda$	5e-5	1e-4	5e-3	5e-3	5e-3	5e-3	1e-4	5e-3	5e-3	5e-3	5e-3	1e-4	5e-3	5e-3	5e-3
$B$	350	200	150	400	320	350	200	150	400	240	350	200	150	400	240
$\delta^{(-)}$	0.1	0	0	0.01	0	0.1	0	0	0	0.1	0	0	0.05	0.1	0.01
$\delta^{(+)}$	0.05	0.02	0	0.3	0.05	0.05	0.01	0.3	0.01	0	0.01	0.1	0.1	0.01	0
$\bar{\phi}$	3	3	5	3	3	3	3	5	3	3	3	3	3	3	3
#epochs	20	15	30	30	20	20	15	30	30	30	100	100	100	100	20

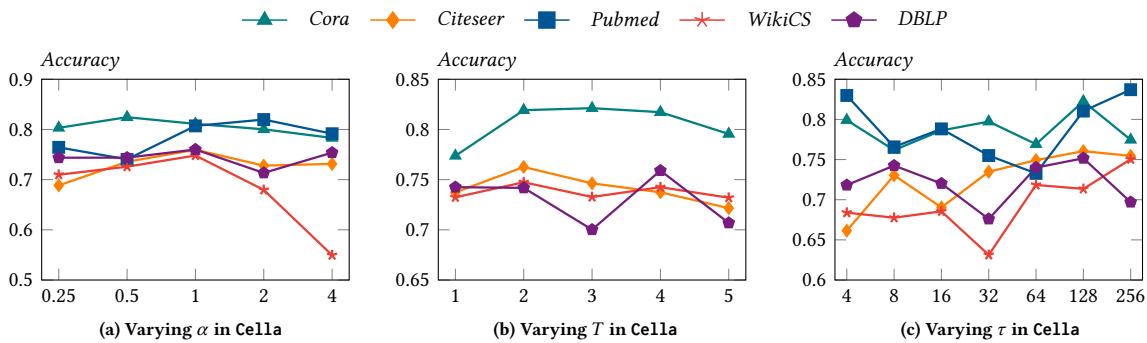


**Figure 5: Varying parameters in Cella.**

**B.2 Datasets and Metrics**

*Cora*, *Citeseer* and *Pubmed* are three widely used datasets in the GNN community. Each node indicates a paper, and the edges indicate the citation relation. We get the raw text of each paper from [6]. *Wiki-CS* consists of nodes corresponding to Computer Science articles, with edges based on hyperlinks and 10 classes representing

different branches of the field [45]. More details can be found in Table 6. About the metrics, NMI measures the information shared between the predicted label and the ground truth. When data are partitioned perfectly, the NMI score is 1, while it becomes 0 when prediction and ground truth are independent. ARI is a metric to measure the degree of agreement between the cluster and golden

**Table 8: Comparison with clustering approaches.**

Method	Cora				CiteSeer				PubMed				WikiCS				DBLP			
	Acc	NMI	ARI	F1	Acc	NMI	ARI	F1	Acc	NMI	ARI	F1	Acc	NMI	ARI	F1	Acc	NMI	ARI	F1
AGC-DRR [16]	66.97	53.66	46.14	63.21	69.56	48.54	49.42	65.97	<u>65.87</u>	25.10	<u>25.78</u>	65.48	57.17	46.06	39.89	48.46	74.04	<b>44.17</b>	45.98	72.66
AGCN [46]	62.88	47.79	35.82	53.86	61.45	40.79	37.15	54.97	65.09	26.39	25.59	<u>65.93</u>	50.38	40.98	32.83	38.13	<u>75.59</u>	43.51	<u>49.67</u>	<u>73.05</u>
CCGC [74]	<u>74.62</u>	<u>56.71</u>	<u>53.86</u>	<u>71.46</u>	49.45	33.23	35.11	44.29	44.16	17.74	17.68	44.14	32.08	21.06	7.66	30.76	72.85	40.92	45.02	70.61
DAEGC [63]	72.62	53.40	49.51	70.06	69.08	47.04	47.55	65.21	62.97	22.61	21.15	63.59	<u>59.09</u>	<u>47.30</u>	<u>45.72</u>	<u>52.64</u>	75.04	43.70	48.92	72.74
DFCN [58]	70.10	50.57	44.61	66.13	71.12	<u>48.65</u>	50.89	<b>66.46</b>	62.68	<u>22.94</u>	21.28	63.28	52.89	43.75	30.57	40.15	74.74	43.91	48.97	72.37
EFR-DGC [19]	64.55	52.15	43.40	61.47	<u>72.40</u>	48.86	50.14	<u>66.18</u>	62.63	21.99	20.59	63.11	56.70	41.28	41.14	42.98	73.30	41.93	46.93	70.71
GCAE [71]	65.07	51.80	43.50	61.29	74.18	49.27	<u>51.77</u>	67.00	58.15	15.25	13.94	58.02	56.19	48.68	40.61	48.24	72.15	40.59	43.77	70.39
Cella	<b>81.80</b>	<b>64.22</b>	<b>64.30</b>	<b>79.64</b>	<b>76.16</b>	<b>50.87</b>	<b>54.14</b>	65.28	<b>83.70</b>	<b>48.86</b>	<b>56.56</b>	<b>83.26</b>	<b>74.52</b>	<b>54.15</b>	<b>57.37</b>	<b>69.29</b>	<b>76.37</b>	<u>44.14</u>	<b>50.75</b>	<b>74.12</b>
Improv.	7.18	7.51	10.44	8.18	1.98	1.6	2.37	-1.72	17.83	22.47	30.78	17.33	15.43	5.47	11.65	16.65	0.78	-0.03	1.08	1.07

distribution, which ranges in  $[-1,1]$ . The more consistent the two distributions, the higher the score.

### B.3 Hyper-parameter Settings

We present the selection of all hyper-parameters in Table 7. For all GAT-based methods, we follow the settings from [60], where the number of attention heads is set to 8, and the number of output heads is set to 1. Specifically, for the *PubMed* dataset, the number of output heads is set to 8.

For all GCNII-based methods, we adhere to the settings outlined in [5]. In particular, for *Cora*, the number of layers is set to 64, for *Citeseer* the number of layers is 32, and for *WikiCS* and *PubMed*, the number of layers is 16.

## C Additional Experiment Results

### C.1 More Hyper-parameter Analysis

In this section, we further analyze the effect of  $\alpha$ ,  $T$ , and  $\tau$ . These parameters are crucial for the initial active selection process introduced in Section 4.2. We investigate the impact of each parameter and present the results in Figure 5. The results indicate that varying  $\tau$  has the most significant effect on overall performance, particularly on the *WikiCS* dataset.

$T$  and  $\alpha$  are two factors in Eq. (3) that represent the depth of the encoded representations and the importance of each hop. As shown in Figure 5(b), in most cases, setting  $T = 2$  and  $\alpha = 1$  is sufficient to achieve excellent results.

### C.2 Cost Analysis of Cella

In this section, we first analyze the training time of various LLM-GNN [7] variants and Cella, as presented in Table 9. As shown, Cella is at least  $2\times$  faster than the best-performing variant of the state-of-the-art LLM-GNN, namely LLM-GNN (RIM). While LLM-GNN (Featprop) and LLM-GNN (Graphpart) adopt faster active node selection strategies, they sacrifice accuracy for speed. In contrast, although Cella introduces additional training steps, its active node selection approach, as described in Sec. 4.2.1, achieves high effectiveness with relatively low computational cost. In comparison, the label selection process in LLM-GNN (RIM) relies on an iterative batch setting, which is more computationally expensive.

Moreover, we conduct an experiment to evaluate the financial query costs associated with Cella, as well as the overall dataset, which are presented in Table 10. The cost is calculated based on the tokenizer of GPT-3.5-turbo and OpenAI’s official pricing.

### C.3 Comparison with Graph Clustering Methods

Label-free node classification is similar to Clustering, with the key distinction being the use of external category information. Clustering methods can be evaluated by mapping the predicted clustering assignment vector to the ground truth labels using the Kuhn-Munkres algorithm [47].

In Table 8, we present the performance of various clustering methods across the five datasets and compare them with Cella. We highlight the best result in bold and the runner-up with an underline. The results demonstrate that Cella outperforms all clustering methods, achieving an improvement in accuracy of up to 17.83%. These findings highlight the superiority of the proposed pipeline over traditional clustering approaches.

**Table 9: Runtime Cost (sec) Analysis of Cella**

	LLM-GNN (FeatProp)	LLM-GNN (Graphpart)	LLM-GNN (RIM)	Cella
<i>Cora</i>	26.8	40.4	141.9	50.9
<i>Pubmed</i>	39.4	53.2	776.8	217.6
<i>WikiCS</i>	52.2	60.1	934.7	217.1
<i>DBLP</i>	72.5	46.5	500.2	208.7

**Table 10: Monetary Cost (US\$) Analysis of Cella**

	Cella	Total
<i>Cora</i>	0.10\$	1.33\$
<i>Citeseer</i>	0.07\$	1.81\$
<i>Pubmed</i>	0.09\$	21.83\$
<i>WikiCS</i>	0.35\$	18.65\$
<i>DBLP</i>	0.01\$	0.50\$

**Table 11: Performance of Cella with GPT-3.5-turbo, GPT-4-turbo and GPT-4o.**

	<i>Cora</i>	<i>Citeseer</i>
Cella (GCN) with GPT-3.5-turbo	<b>81.80</b>	<b>76.16</b>
Cella (GCN) with GPT-4-turbo	79.50	74.79
Cella (GCN) with GPT-4o	80.21	74.87
Cella (GAT) with GPT-3.5-turbo	76.06	73.97
Cella (GAT) with GPT-4-turbo	77.95	74.52
Cella (GAT) with GPT-4o	75.94	73.53
Cella (GCNII) with GPT-3.5-turbo	78.71	73.14
Cella (GCNII) with GPT-4-turbo	77.83	71.39
Cella (GCNII) with GPT-4o	76.99	70.39

**Table 12: Ablation Study on Active Node Selection in Cella**

	Cella ( <i>K</i> -Means)	Cella	Improv.
<b><i>Cora</i></b>	73.83	81.80	7.97
<b><i>Citeseer</i></b>	67.05	76.16	9.11
<b><i>Pubmed</i></b>	71.58	83.70	12.12
<b><i>WikiCS</i></b>	65.26	75.23	9.97
<b><i>DBLP</i></b>	73.21	75.55	2.34

**Table 13: Accuracy of LLM-generated Annotations**

<b><i>Cora</i></b>	<b><i>Citeseer</i></b>	<b><i>DBLP</i></b>
73.7	74.0	75.0

**Table 14: Cella with Ground-truth Annotations**

	Cella	Cella (ground-truth)
<b><i>Cora</i></b>	81.8	84.7
<b><i>Citeseer</i></b>	76.1	76.2
<b><i>DBLP</i></b>	75.6	78.8

#### C.4 Evaluating Cella with More GPT Models

We also conducted an experiment using more advanced models, GPT-4 and GPT-4o, to annotate labels and perform the task of node classification. The results are presented in Table 11. Interestingly, in some cases, Cella with noisier labels produced by GPT-3.5-turbo outperforms the higher-quality labels generated by GPT-4-turbo or GPT-4o. This indicates that, with the assistance of Cella, the performance of the LLM is no longer the sole bottleneck in zero-shot node classification. Even when using a weaker model, we can achieve results comparable to those of a stronger model, while the query costs between weaker and stronger models can differ by orders of magnitude.

#### C.5 Ablation Study on Active Node Selection

To verify the efficacy of our subspace clustering technique for active node selection in Section 4.2.1, we substitute *K*-Means for it in Cella. As reported in Table 12, the variant of Cella with *K*-Mean consistently exhibits remarkable performance degradation compared to the version using the subspace clustering. For example, on the *Pubmed* dataset, the subspace clustering approach attains a large margin of 12.12% in terms of classification accuracy compared to *K*-Means. The reason is that *K*-Means tends to group the majority of nodes into only a few clusters, making it hard to select sufficient representative nodes for annotation. In contrast, as elaborated in Section 4.2.1, our subspace clustering approach can filter out the noise and identify the inherent structure underlying the node features for a more balanced partition.

#### C.6 Ablation Study on LLM-based Annotations

This section empirically studies the quality of LLM-generated node annotations that are used for training. First, on three representative datasets *Cora*, *CiteSeer*, and *DBLP*, the LLM-generated annotations, i.e., the pseudo-labels of nodes output by the LLM, are of an accuracy of around 75%, as reported in Table 13. However, Table 14 shows that our Cella model trained using such LLM-generated pseudo-labels is able to achieve competitive classification performance when compared to that by Cella trained with the ground-truth labels. Particularly, on the *CiteSeer* dataset, both versions achieve a classification accuracy of 76.1% and 76.2%, respectively. The results manifest the strong effectiveness of the self-training architecture, informative sample selection and hybrid label refinement modules in our Cella.